JOURNAL OF GEOPHYSICAL RESEARCH, VOL. 103, NO. B11, PAGES 26,869-26,883, NOVEMBER 10, 1998

Nonlinear sediment response during the 1994 Northridge earthquake: Observations and finite source simulations

Edward H. Field,[1] Yuehua Zeng,[2] Paul A. Johnson,[3] and Igor A. Beresnev[4]

Abstract. We have addressed the long-standing question regarding nonlinear sediment response in the Los Angeles region by testing whether sediment amplification was similar between the Northridge earthquake and its aftershocks. Comparing the weak- and strong-motion site response at 15 sediment sites, we find that amplification factors were significantly less for the main shock implying systematic nonlinearity. The difference is largest between 2 and 4 Hz (a factor of 2), and is significant at the 99% confidence level between 0.8 and 5.5 Hz. The inference of nonlinearity is robust with respect to the removal of possibly anomalous sediment sites and how the reference-site motion is defined. Furthermore, theoretical ground-motion simulations show no evidence of any bias from finite source effects during the main shock. Nonlinearity is also suggested by the fact that the four sediment sites that contain a clear fundamental resonance for the weak motion exhibit a conspicuous absence of the peak in the strong motion. Although we have taken the first step of establishing the presence of nonlinearity, it remains to define the physics of nonlinear response and to test the methodologies presently applied routinely in engineering practice. The inference of nonlinearity implies that care must be exercised in using sediment site data to study large earthquakes or predict strong ground motion.

1. Introduction

It has been recognized since at least 1898 [*Milne*, 1898] that sedimentary deposits can increase earthquake ground motion relative to bedrock. Such sediment amplification has been documented in numerous studies of small earthquakes, and the physics is well understood in terms of linear elasticity [*Aki*, 1988]. In order to conserve energy, wave amplitudes generally increase in sediments due to lower seismic velocities and densities. In addition, resonances can occur where distinct layer boundaries exist.

For the damaging levels of ground motion produced by large earthquakes, however, there has been a long-standing debate regarding the nature of sediment amplification. The prevailing view in the geotechnical engineering community is that sediments behave nonlinearly during large earthquakes [e.g., *Hardin and Drnevich*, 1972a,b; *Finn*, 1991; *Ishihara*, 1996]. That is, due to the finite strength of unconsolidated sediments, the shear modulus depends on the strain amplitude in violation of Hooke's law. This perspective is based almost entirely on laboratory tests of sedimentary samples, which imply that the shear modulus (and thus the shear wave velocity) is reduced, and the degree of attenuation (or damping) is increased as strain amplitudes increase [e.g., *Hardin and Drnevich*, 1972b; *Vucetic and Dobry*, 1991]. This predicts a nonlinear response where the degree of amplification generally decreases, and layer resonances shift to lower frequencies, as the level of ground motion increases. In fact, at some point sediments are believed to reduce amplitudes relative to bedrock [e.g., *Seed and Idriss*, 1983; *Idriss*, 1990]. A large body of engineering literature exists on this topic, upon which methodologies have been developed and used in practice since the 1970s [e.g., *Ishihara*, 1996]. Unfortunately, these methodologies are not based on any fundamental principles of physics. In fact, according to a recently published engineering textbook on the subject [*Ishihara*, 1996, p. 28] "...there is no nonlinear model of any kind established on a sound physical basis."

Short of the quicksand effect of liquefaction, where water-saturated sands loose shear rigidity and behave as a liquid [*Seed and Lee*, 1966; *Ishihara*, 1996], seismologists have traditionally remained skeptical as to the pervasiveness of nonlinear sediment behavior. Their reasons were: (1) a reluctance to introduce a significantly more complicated model, and a desire to err on the side of caution, when the relatively few strong-motion observations were consistent with linear elasticity; (2) a skepticism that laboratory measurements can reliably reflect in situ behavior given the well-known difficulties of obtaining undisturbed sediment samples for analysis. This seismological perspective was reflected in a 1988 seminal review [*Aki*, 1988, p. 115] which concluded that "... the amplification factor obtained for a given site using weak motion data can be used to predict the first order effect on strong ground motion ...." This assertion was supported by the observation that the lake bed clays in Mexico city generally behaved linearly during the 1985 Michoachan earthquake [*Aki*, 1993], which contributed to the collapse of more than 300 buildings [*Celebi et al.*, 1987].

As reviewed by *Aki* [1993], and more thoroughly by *Beresnev and Wen* [1996], scattered seismological evidence of sediment nonlinearity has emerged from more recent

[1]Department of Earth Sciences, University of Southern California, Los Angeles
[2]Seismological Laboratory, University of Nevada, Reno.
[3]Los Alamos National Laboratory, Los Alamos, New Mexico.
[4]Department of Earth Sciences, Carleton University, Ottawa, Ontario, Canada.

Paper Number 98JB02235.
0148-0227/98/98JB-02235$09.00

earthquakes. However, many of these are thought to be associated with liquefaction, such as the observations at Treasure Island during the 1989 Loma Prieta earthquake [e.g., *Jarpe et al.*, 1989] and at Port Island in Kobe, Japan during the 1995 Hyogoken-Nanbu earthquake [e.g., *Kazama*, 1996; *Aguirre and Irikura*, 1995]. In addition, some of the studies have been challenged in the literature and remain controversial [e.g., *Chin and Aki*, 1991; *Wennerberg*, 1996; *Chin and Aki*, 1996a].

The significance of nonlinearity for the type of stiff-soil sites found in southern California remains particularly problematic. *Rogers et al.* [1984] reported no statistically significant evidence for nonlinear sediment response in the Los Angeles basin during the 1971 San Fernando earthquake, although *Beresnev and Wen* [1996] have suggested that their analysis was not ideally suited for such a test. In addition, studies of observed and predicted peak motion during the 1994 Northridge earthquake have resulted in mixed interpretations [*Borcherdt*, 1996; *Chin and Aki*, 1996b], and a study by *Harmsen* [1997] of spectral amplification was nonconclusive. This lack of strong evidence for sediment nonlinearity in the greater Los Angeles region could be due either to it not being significant for the levels of ground motion thus far experienced or to it having gone undetected given other sources of uncertainty in the data.

The present disparity between seismological understanding and engineering practice for sediment sites in southern California remains a significant impediment to the further refinement of seismic hazard assessments, as reflected in a recent study where some of the ground motion models applied assumed nonlinearity and some did not [*Petersen et al.*, 1997]. The issue of nonlinearity also brings into question the use of empirical Greens functions [*Bakun and Bufe*, 1975; *Mueller*, 1985] as an estimate of combined path and site effects at sediment sites during large earthquakes. Given the limited quantity of strong-motion data that currently exists, an appropriate strategy of addressing this problem is to develop novel ways of analyzing existing data.

Previously *Field et al.* [1997] presented preliminary evidence for a systematic nonlinear response at sediment sites during the 1994 Northridge earthquake. We extend those results here by applying a more elaborate set of statistical tests. Most importantly, we present theoretical ground motion simulation results to demonstrate that finite source effects do not influence the inference of sediment nonlinearity. Our primary goal here is to firmly establish the presence of sediment nonlinearity, leaving any detailed quantification of the physical process or testing of engineering methodologies to subsequent studies.

2. Seismic Data

In order to make a systematic comparison of site response estimates between strong and weak motion, we compiled data for all sites where both Northridge main shock and aftershock recordings were obtained. After excluding one site (Tarzana) because of unexplained anomalous behavior [*Chang et al.*, 1996; *Spudich et al.*, 1996; *Rial*, 1996], we were left with the 21 sites listed in Table 1 and plotted in Figure 1. We will refer to sites by their strong-motion station name (see Table 1 for the name of the colocated aftershock recording site). On the basis of surface geology, 15 of these sites are categorized as sediments (Quaternary alluvium), 2 as soft rock (Tertiary units), and 4 as hard rock (Mesozoic basement).

To keep the quantity of data manageable, we have limited ourselves to aftershocks greater than magnitude 3.0 which occurred within 20 days of the main shock and that were recorded at the hard-rock site SCT. The 184 resultant events are plotted in Figure 1 (a complete list, as well as the waveform data, are available from E. H. Field). Also shown in Figure 1 is the surface projection of the main shock rupture distribution as determined by *Wald et al.* [1996].

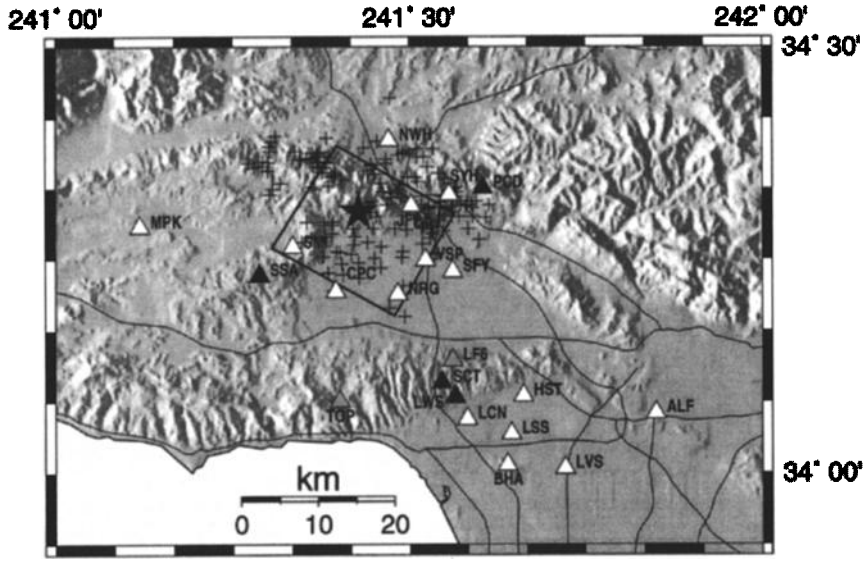

Figure 1. Relief map of the study region. The alluvium recording sites are shown as white triangles, the soft rock sites are shown as gray triangles, and the hard rock sites are shown as black triangles. Aftershocks epicenters are shown with crosses, and the main shock rupture distribution is outlined by the box [*Wald et al.*, 1996]. The fault plane dips to the southwest, with the top edge at a depth of 5 km and the bottom edge at a depth of 20.4 km. The location of maximum slip is marked with the solid star. See Table 1 for station names. Reprinted by permission from *Nature* [Field et al., 1997, Copyright 1997, Macmillan Magazines Ltd.].

Table 1. Station Information

Strong-Motion Station Information[a]						Colocated Aftershock Recording Site			General Information	
Site Abbreviation	Peak Acceleration cm/s^2	Site Geology	Latitude	Longitude	Source[b]	Site Abbreviation	Source[c]	Number of Aftershocks Recorded	Station Separation m	Ratio at 3 Hz[d]
CPC	538	sediment	34.212	-118.605	USC	CPCP	SCEC	53	0	1.77
JFP	616	sediment	34.313	-118.498	USGS	JFPP	SCEC	32	200	7.98
LCN	251	sediment	34.063	-118.418	CDMG	LA02	SCEC	57	0	1.99
HST	225	sediment	34.090	-118.338	SCEC	LA03	SCEC	91	0	1.40
ALF	99	sediment	34.070	-118.150	CDMG	LA04	SCEC	69	0	1.27
MPK	286	sediment	34.288	-118.881	CDMG	MPKP	SCEC	26	100	1.52
NWH	578	sediment	34.390	-118.530	CDMG	NWHP	SCEC	42	0	2.05
SFY	541	sediment	34.236	-118.439	CDMG	SFYP	SCEC	44	0	2.90
VSP	923	sediment	34.249	-118.478	USGS	VAN	SCEC	5	0	9.37
LVS	285	sediment	34.005	-118.279	USC	WVES	SCEC	6	0	0.91
LSS	482	sediment	34.046	-118.355	USC	SSC	SCEC	2	100	2.52
SYH	827	sediment	34.326	-118.444	CDMG	SYF	USGS	19	0	1.60
BHA	234	sediment	34.009	-118.361	LA	BHG	USGS	15	0	1.83
NRG	468	sediment	34.209	-118.517	USC	WC1	USGS	9	0	2.28
SMI	924	sediment	34.264	-118.666	USC	SMIP	SCEC	36	160	1.28
LF6	498	soft rock	34.132	-118.439	USC	LA01	SCEC	85	0	5.96
TOP	327	soft rock	34.084	-118.599	USGS	TPC	USGS	4	0	1.32
SSA	336	hard rock	34.231	-118.713	DOE	SSAP	SCEC	26	0	1.52
SCT	371	hard rock	34.106	-118.454	SCEC	LA00	SCEC	184	0	0.97
PCD	426	hard rock	34.334	-118.396	CDMG	PDAM	SCEC	25	200	0.42
LWS	293	hard rock	34.089	-118.435	USC	HWS	USGS	14	200	1.61

[a]Data and information come from the Strong-Motion Database of the Southern California Earthquake Center (http://quake.crustal.ucsb.edu/scec/smdb/smdb.html).

[b]The original sources of data are as follows: USC, University of Southern California; SCEC, Southern California Earthquake Center; CDMG, California Division of Mines and Geology; USGS, U. S. Geological Survey; DOE, Department of Energy; LA, City of Los Angeles.

[c]The aftershock data sources are as follows: SCEC, from the Southern California Earthquake Center Data Center (http://www.scecdc.scec.org) or [*Edelman and Vernon*, 1995]; USGS, from the United States Geological Survey [*Meremonte et al.*, 1996].

[d]The ratio of weak to strong motion site response estimate (as plotted in Figure 4) at 3 Hz.

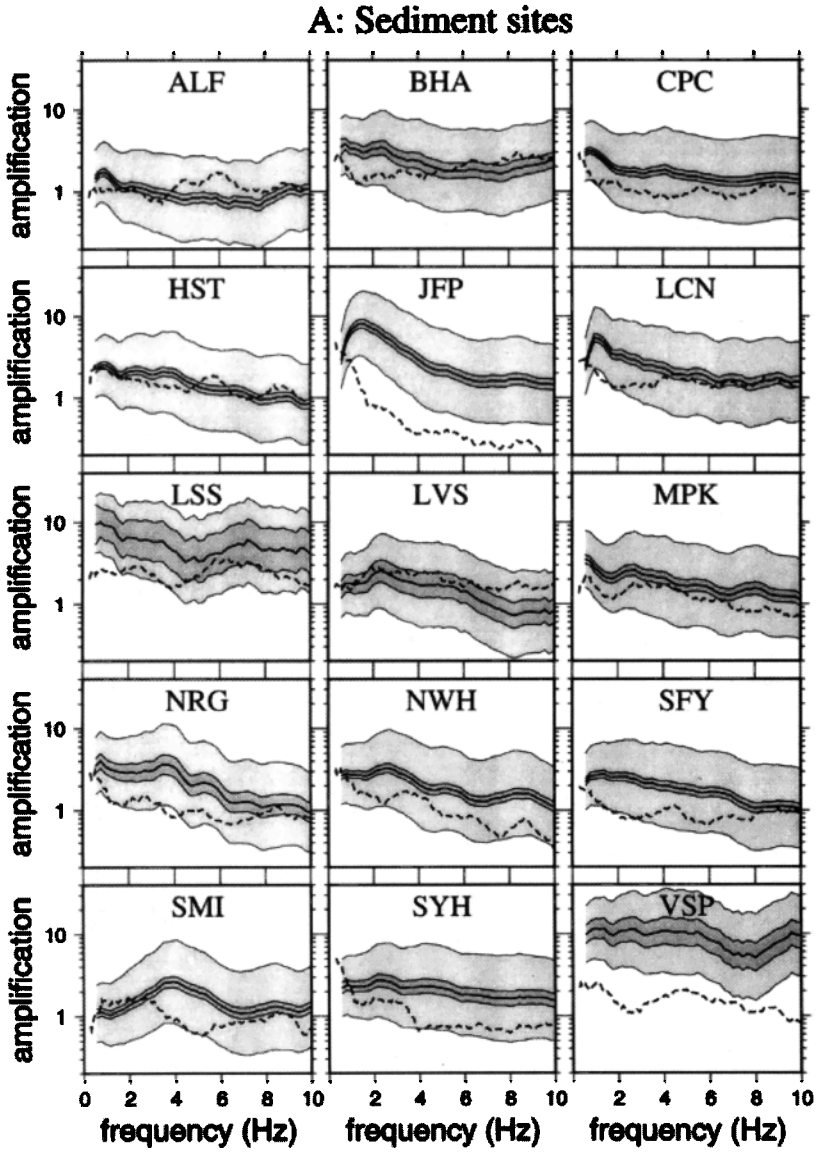

Figure 2. The site response estimates for (a) the 15 sediment sites, (b) the four hard-rock (Mesozoic basement) sites, and (c) the two soft-rock (Tertiary) sites. The weak-motion estimates obtained from the aftershocks are plotted with the solid lines. The lighter shading represent ±2 standard deviations, representing the range where approximately 95% of the individual estimates reside. The darker shading represents the approximate 95% confidence limits of the mean. The strong-motion site-response estimates obtained from the main shock data are plotted with the dashed lines. The lower-frequency cutoffs represent limits imposed by noise and instrument limitations as outlined in the Appendix.

The levels of peak ground accelerations experienced during the main shock were between 293 and 426 cm/s^2 at the hard-rock sites and between 99 and 924 cm/s^2 at the sediment sites (Table 1). For comparison, the peak ground accelerations experienced at the hard-rock site SCT ranged between 0.18 and 55.54 cm/s^2 for the aftershocks.

3. Site Response Estimation

3.1. Weak Motion

Following the work of several previous investigators [e.g., *Borcherdt*, 1970; *Andrews*, 1986; *Bonamassa and Mueller*, 1989; *Boatwright et al.*, 1991], the horizontal component shear wave Fourier amplitude spectrum observed at the ith site for the jth aftershock, $O_{ij}(f)$, is represented as a product of source, path, and site effects:

$$O_{ij}(f) = E_j(f)\, P_{ij}(f)\, S_i(f) \qquad (1)$$

where f is frequency, $E_j(f)$ is the source effect of the jth event, $P_{ij}(f)$ is the path effect for the ith station and jth event, and $S_i(f)$ is the site response for the ith site. The path effect is further specified as

$$P_{ij}(f) = r^{-1}\, e^{-\pi f T_s / Q(f)} \qquad (2)$$

where r is the hypocentral distance measured from the aftershock location, T_s is the observed shear wave travel time, and $Q(f)$ is an assumed quality factor representing attenuation.

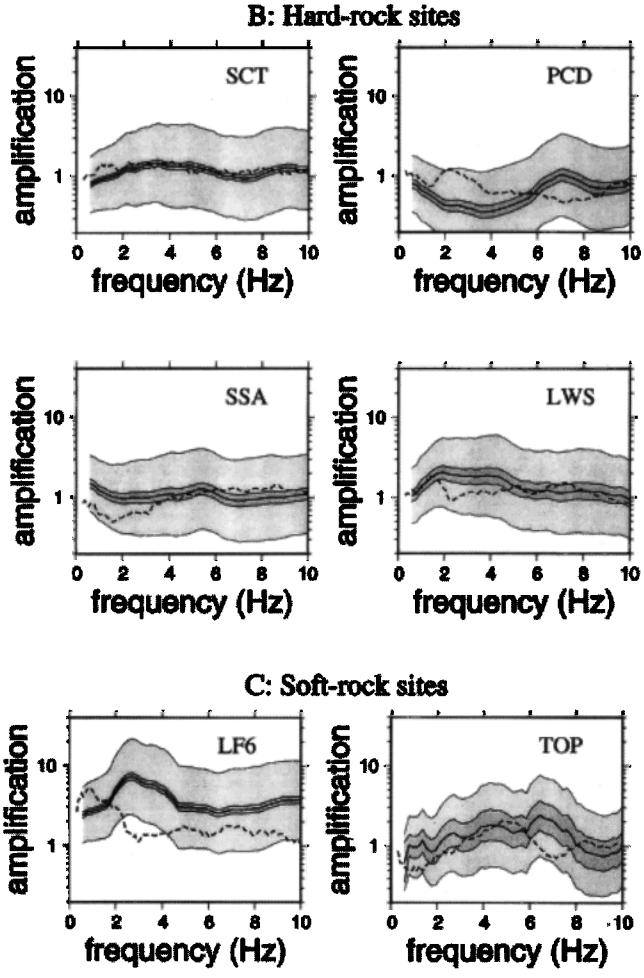

Figure 2. (continued)

By taking the logarithm of both sides of equation (1), all aftershock source effects ($E_j(f)$) and all site response estimates ($S_i(f)$) are solved for simultaneously using a linear least squares generalized inversion [*Andrews*, 1986]. Of the many schemes that have been proposed, we follow that outlined by *Field and Jacob* [1995] to ensure reliable uncertainty estimates. There is one unconstrained degree of freedom in the inversion which means that all site response estimates can be multiplied by an arbitrary value provided all source effects are divided by the same amount. This is constrained by stipulating that one or more of the rock sites, referred to as the reference motion, has no site response on average (i.e., unit amplification). The resultant site-response estimates therefore represent path-effect-corrected average sediment-to-bedrock spectral ratios.

The weak-motion site-response estimates obtained from the aftershock data are presented in Figure 2a for the 15 sediment sites, Figure 2b for the four hard-rock sites (Mesozoic basement), and Figure 2c for the two soft-rock (Tertiary) sites. Following *Hartzell et al.* [1996], we have assumed that $Q(f) = 150f^{0.5}$ in the path-effect correction. The inversion constraint has been applied as the average of all hard-rock sites being equal to unity, meaning the estimates are relative to the average site response at the four hard-rock sites (PCD, SCT, LWS, and SSA). The estimation technique used to compute the horizontal component spectra is detailed the Appendix, and the uncertainties have been obtained assuming a lognormal distribution as legitimized by *Field and Jacob* [1995].

Some of the weak-motion estimates shown in Figure 2 can be compared with the results found in other studies. Specifically, the response for sites CPC, JFP, LF6, MPK, NWH, PCD, SMI, SSA, and SCT compare favorably with those found by *Bonilla et al.* [1997], in spite of different spectral estimation techniques, path-effect corrections, and reference-site definitions. Similarly, the results for sites VSP, LSS, TOP, SYH, BHA, NRG, and LWS generally agree with those found by *Hartzell et al.* [1996], although the comparison is more difficult since they did not provide uncertainty bounds. Finally, the response for site LF6 agrees with the traditional sediment-to-bedrock spectral ratio (LF6/LWS) computed by Beresnev et al. (1998a).

3.2. Strong Motion

The strong-motion site-response estimates are plotted in Figure 2 with the dashed lines. These were obtained from the main shock data using equations (1) and (2) exactly as was done for the weak-motion aftershocks. However, care has been taken in defining the hypocentral distance r because the spatial distribution of rupture (18 by 24 km according to *Wald et al.* [1996]) was a significant fraction of the distance to each site. Care was also taken in defining T_s because the rupture persisted for several seconds. Therefore r and T_s were defined relative to the location and timing of maximum moment release as determined by *Wald et al.* [1996], which ruptured 4.5 s into the total rupture duration of 7 s. This point is marked as a star in Figure 1. With these values it is presumed that the effects of energy arriving from distances nearer and farther than r, as well as before and after T_s, have been averaged out. As discussed later, this assumption has been tested.

With the strong-motion estimates we also need to consider other finite source effects such as rupture directivity [e.g., *Archuleta and Hartzell*, 1981; *Heaton*, 1982, 1990]. These result from the large spatial extent of the main shock, where energy arriving from different locations on the fault plane may interfere constructively or destructively, causing $E_j(f)$ to vary with site location. To the extent that both the sediment and hard-rock sites exhibit a good spatial distribution about the main shock, these finite source effects will presumably be averaged out. Nevertheless, we explicitly test for any potential biases introduced by finite source effects later in this paper.

3.3. Comparison of Weak and Strong Motion Estimates

It is important to note that any systematic differences between the true path effect and that assumed in equation (2), as well as any site effect in the reference-site definition, has been mapped onto the site-response estimates as a source of bias. Therefore we caution against inferring the "true response" or absolute amplification levels at any particular site. However, since the main shock and aftershocks traveled similar paths, and the same reference-site definition has been applied in both cases, the weak- and strong-motion estimates should be equally biased.

Except for two cases (VSP and JFP), the strong-motion site-response estimates plotted in Figure 2 (dashed lines) generally fall within the natural variability of the weak motion

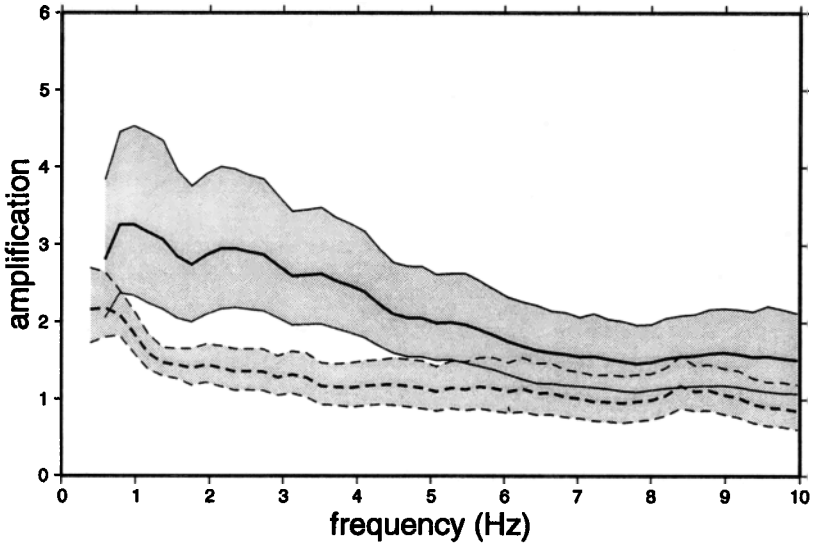

Figure 3. The mean and ±2 standard deviation of the mean confidence limits for the 15 alluvium site-amplification estimates. The solid lines represent the weak-motion results for the aftershocks, and the dashed lines represent the strong-motion results for the main shock. Reprinted by permission from *Nature* [Field et al., 1997, Copyright 1997, Macmillan Magazines Ltd.].

estimates (±2 standard deviations as represented by the lightly shaded region). That is, the individual site response estimates do not suggest statistically significant nonlinearity. The level of variability exhibited by the weak-motion estimates is precisely why it has been difficult to resolve the issue of nonlinearity in previous studies. However, we now have results for several sediment sites which can be combined to see if any systematic nonlinear behavior is identifiable.

Shown in Figure 3, for the weak- and strong-motion separately, are the mean and approximate 95% confidence limits of the 15 sediment site-response estimates. The average weak-motion sediment amplification is ~3.1 at 1 Hz, ~2.5 at 3 Hz, and ~1.4 at 10 Hz. The strong-motion amplification factors are significantly lower, being 1.9 at 1 Hz, 1.3 at 3 Hz, and 0.8 (deamplification) at 10 Hz. This difference implies the response at sediment sites was, on average, nonlinear, or that significant finite source effects are present.

A more statistically efficient way to look for nonlinearity is to divide the weak- and strong-motion estimates at each site before computing the averages. That way any path-effect or reference-site biases are normalized out. We can then define

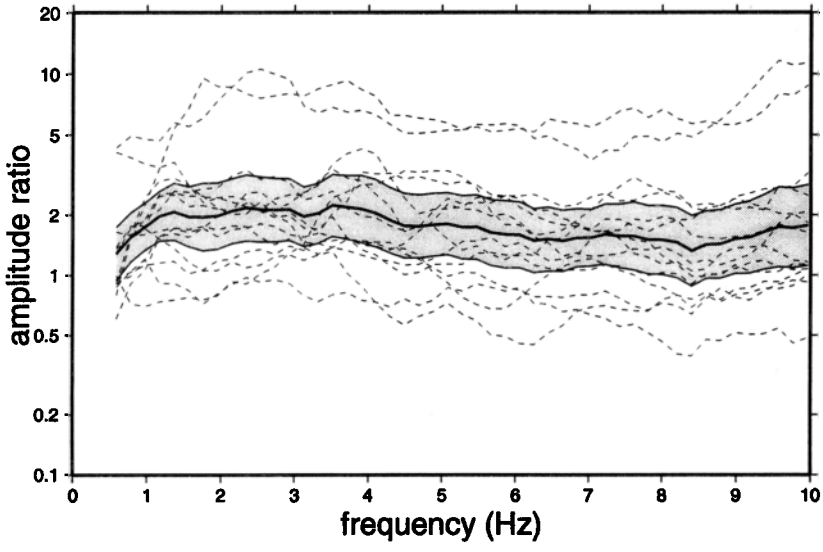

Figure 4. Ratios of the weak- to the strong-motion site response estimates for each of the 15 sediment sites (dashed lines). The values at 3 Hz are listed in Table 1. The mean and 95% confidence region of all the sediment-site ratios are plotted with the solid lines and shaded region (based on a t distribution with 14 degrees of freedom), revealing that the weak-motion amplification estimates are, on average, significantly higher implying nonlinearity. Reprinted by permission from *Nature* [Field et al., 1997, Copyright 1997, Macmillan Magazines Ltd.].

the null hypothesis that the weak- and strong-motion response was similar and test this by determining whether the ratios are significantly different from unity. The result is shown in Figure 4, where the individual ratios are plotted with a dashed line and the mean and 95% confidence region is plotted with the solid lines and shaded region. The result implies that the weak-motion response is significantly greater (at the 95% level of confidence) over almost the entire frequency band, leading to the rejection of the null hypothesis that the response was linear. In fact, the difference is significant at the 99% confidence level between 0.8 and 5.5 Hz. We have conducted several tests to ensure that the difference seen in Figure 4 does not result from something other than nonlinearity. These are discussed in section 4.

4. Tests of Potential Biases

Figure 4 exhibits two ratios that have particularly high values. One might wonder therefore if the rejection of the null hypothesis depends on the inclusion of these two anomalous sites. The average difference in Figure 4 is largest between 2 and 4 Hz, so consider the ratio values at 3 Hz (listed in Table 1 for reference). If we exclude the two highest values (corresponding to VSP and JFP as seen in Figure 2 and Table 1), the difference actually becomes more significant as the standard deviation is reduced more than the mean. In fact, at 3 Hz one must remove the 10 highest ratios in Figure 4 before the difference loses significance at the 95% confidence level (according to the t distribution). Therefore it does not seem likely that the result is biased by the inclusion of a few possibly anomalous sediment sites.

Similarly, one might suspect that the inclusion of an anomalous hard-rock site in the reference-motion definition could bias the result. As stated previously, the absolute amplification levels (e.g., Figure 3) do indeed depend on which combination of rock sites is used as the reference. This can be seen by examining the individual hard-rock site-response estimates plotted in Figure 2b. However, the difference between the weak- and strong-motion estimates, in terms of rejecting the null hypothesis as plotted in Figure 4, does not depend on the inclusion of any particular rock site. In fact, we found that the difference persists no matter what combination of hard-rock sites is used as the reference motion. Therefore the conclusion of significant nonlinearity is unlikely to be biased by any anomalies at the hard-rock sites.

To test whether the choice of quality factor applied in equation (2) ($Q(f) = 150f^{0.5}$ [from *Hartzell et al.*, 1996]) might influence out result, we also applied the Q models of *Peng* [1989] and *Bonillia et al.* [1997], as well as a constant Q of 328 (obtained by including this as a parameter to be solved for in the inversion) and found the results unchanged. This is not unexpected since, as discussed above, taking the ratios of weak- to strong-motion site response as in Figure 4 should normalize any path-effect biases out.

The shallowest depth of the main shock rupture was about 5 km, with the most significant moment release below 7 km [*Wald et al.*, 1996]. One might therefore wonder if including aftershocks with significantly shallower depths introduces a bias. To test this possibility, we also performed the inversion using only aftershocks of depth greater than 7 km. The result, plotted in Figure 5, does not change the conclusion regarding the null hypothesis. This test also rules out a possible bias from the earliest aftershocks that were assigned a nominal depth of 6 km.

4.1. Finite Source Effects

Perhaps the most severe potential source of bias comes from finite source effects which, as stated previously, result from the large spatial extent of the main-shock rupture. To test whether our choice of hypocentral distance (r), as measured from the location of maximum moment release (star in Figure 1), might be influential, we also defined the hypocentral distance from each of the four corners of the fault plane (box in Figure 1) and found the rejection of the null hypothesis unchanged. Similarly, we also defined the travel time T_s relative the initiation and termination of rupture 7 s later, rather than the timing of maximum moment release used above, and came to the same conclusion.

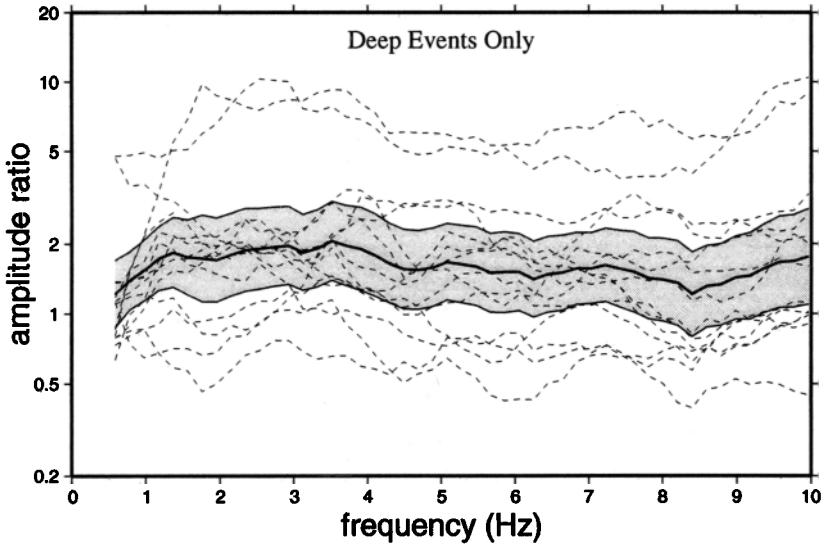

Figure 5. Same as Figure 4, except where only aftershocks with depth greater than 7 km have been used in the inversion.

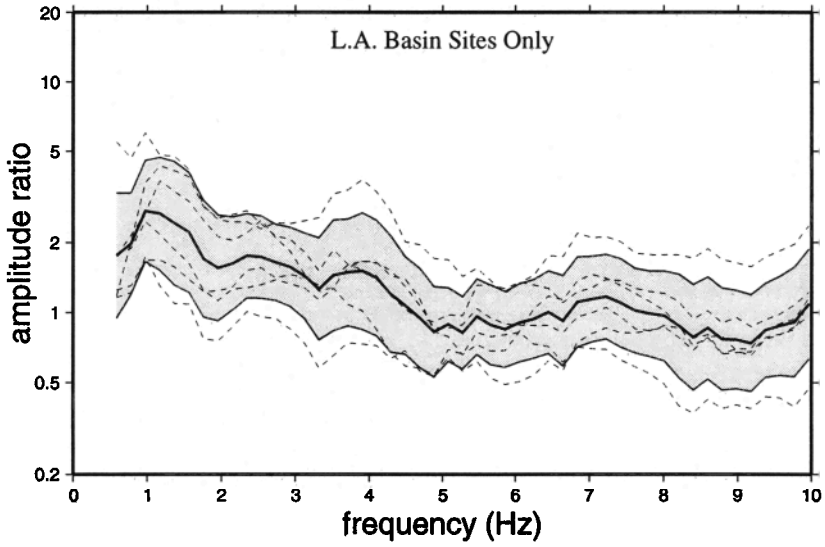

Figure 6. Same as Figure 4, except that only the LA basin sites (LCN, HST, LSS, ALF, BHA, and LVS have been used in the inversion (relative to rock site SCT). Note that the 95% confidence limits here are base on the t distribution with only 5 degrees of freedom (since only six sediment sites are included). The discrepancy at 3 Hz is 1.6 and is significant at the 95% level.

A more problematic finite source effect is produced by rupture directivity [e.g., *Archuleta and Hartzell*, 1981; *Heaton*, 1990; *Somerville et al.*, 1997]. As mentioned previously, this results from the large spatial extent of the rupture, where energy arriving from different locations on the fault plane can interfere constructively or destructively depending on the position of the observational site (causing $E_j(f)$ in equation (1) to vary with location). The Northridge earthquake rupture initiated near the bottom of the fault and propagated updip [*Wald et al.*, 1996]. Because the rupture velocity is similar to the shear wave velocity, waves radiated from different locations on the fault arrived more or less simultaneously for sites located near the updip extension of the fault plane (NWH, JFP, and SYH). This may have caused shorter durations and larger amplitudes, especially at lower frequencies where the energy constructively interferes, relative to the ground motion experienced at other sites. Studies to date suggest that directivity effects are significant at frequencies lower than ~1.6 Hz and generally in the direction perpendicular to the fault plane [*Somerville et al.*, 1997]. This would imply that such effects are probably not influential at the higher frequencies where we infer nonlinearity. However, the data available to study directivity are very limited, so our current understanding may not justify such heuristic reasoning. Therefore it is important to consider how rupture details may have influenced the source effect perceived at each site and how this may influence our inference of nonlinearity.

As one test, we also performed the inversion using only the relatively distant Los Angeles basin sites (LCN, HST, LSS, ALF, BHA, and LVS), with the hard-rock site SCT used as the reference motion. Because these sites are at a greater distance and cover a narrower range of azimuths, any bias due to finite source effects should be reduced. The result is shown in Figure 6. Although we now have only six sites with which to test the null hypothesis, the difference is still significant at 3 Hz at the 95% confidence level. The difference is generally less, a factor of ~1.6 at 3 Hz as opposed to a factor of ~2 in Figure 4, which is consistent with the notion that the nonlinearity will be less for the lower ground motion levels at the more distant sites.

As a more direct and quantitative test, we also investigated the influence of finite source effects by forward modeling the

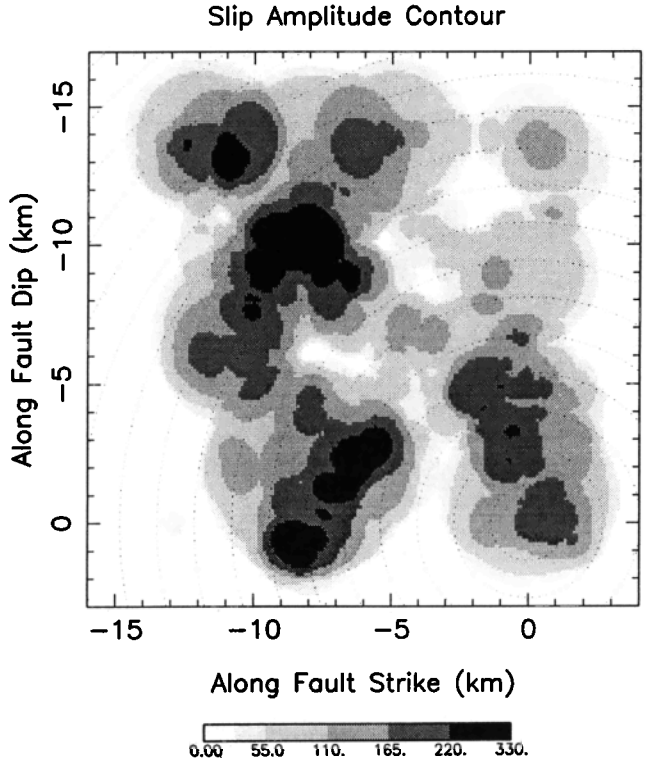

Figure 7. The Northridge earthquake net slip distribution, reproduced from *Zeng and Anderson* [1996], used to compute the main shock synthetic seismograms. The dotted lines are contours of rupture time at 0.5-s intervals.

Table 2. Layered Velocity Model for the Northridge Earthquake Synthetic Seismograms[a]

Thickness, km	V_p, km/sec	Q_p	V_s, km/sec	Q_s	Density
0.1	1.2	50	0.50	20	1.7
0.2	1.9	80	0.95	40	2.0
0.2	2.8	90	1.50	60	2.3
3.5	4.0	600	2.15	400	2.5
2.5	4.8	900	2.65	600	2.6
14.0	6.1	1500	3.50	1000	2.9
16.0	7.0	1500	4.00	1000	3.0
Inf	7.8	1500	4.50	1000	3.3

[a]From *Zeng and Anderson* [1996].

Northridge earthquake ground motion at our 21 sites. We used the kinematic composite source simulation technique of *Zeng et al.* [1994], which represents one of the most extensively validated methodologies available (tested against the Loma Prieta, Landers, and Northridge earthquakes in California, the Guerrero, Mexico earthquake, and the Uttarkashi, India earthquake). The Northridge-specific rupture model obtained by *Zeng and Anderson* [1996] was used here. Specifically, the main shock rupture is represented by a fractal distribution of subevents, each of which radiates the displacement pulse of a crack model [*Sato and Hirasawa*, 1973]. The location and size of each subevent were determined previously by a genetic algorithm inversion of the Northridge earthquake data using frequencies between 0.3 and 3.0 Hz [*Zeng and Anderson*, 1996]. The net slip distribution for this rupture model is shown in Figure 7, which generally agrees with the slip distribution found by others [e.g., *Wald et al.*, 1996]. The Greens functions (i.e., path effects) used in the simulation were computed using the generalized reflection and transmission coefficients method of *Luco and Apsel* [1983]. The same generic southern California velocity model was used for all sites (Table 2), so the synthetic seismograms do not contain site effects. For comparison, a set of synthetics were computed for nine relatively small earthquakes (crack radius of 0.5 km) distributed evenly over the rupture plane, each of which was given the same focal mechanism as the main shock.

An analysis using equations (1) and (2), identical to that applied to the actual observations, was then applied to the synthetic seismograms (with the nine relatively small events representing aftershocks). The resultant site-response estimates for the 15 sediment and 4 hard-rock sites are plotted in Figures 8a and 8b, respectively, in analogy with Figures 2a and 2b. The results for the small earthquakes (solid lines with shading) reveal frequency dependent behavior at some of the sites which might be interpreted as site resonances. However, no site effects were included in the synthetics so this behavior represents differences between the computed Greens functions and the path-effect correction used in the inversion (equation (2)), which is precisely why we previously warned against inferring absolute amplification factors from Figure 2. The results for the main shock synthetics (dashed lines in Figure 8) exhibit some significant differences from the small-event estimates indicating significant finite source effects.

Figure 9 shows the synthetic main shock and small-event site response estimates averaged over the 15 sediment sites. That the average for the small events is near unity over the entire frequency band (i.e., no implied site response) suggests both that equation (2) is an adequate representation, on average, of the theoretical Greens functions and that source radiation pattern effects are averaged out as well. More importantly, the result for the main shock is not significantly different from that of the aftershocks, implying that any finite source effects have also been averaged out and are not masquerading as nonlinearity in the strong-motion observations.

In analogy with Figure 4, Figure 10 shows the ratio of small-event to main shock site response estimates for the synthetic seismograms. The individual estimates reveal some marked departures from unity implying finite source effects. In particular, the three sites that exhibit anomalously low values below 1 Hz (implying relatively high main shock amplitudes due to finite source effects) are JFP, SYH, and NWH. This is a result of the directivity effect described above for these sites located near the updip extension of the fault.

Although the individual ratios in Figure 10 suggest that finite source effects are present, the averages in Figures 9 and 10 suggest that these effects are averaged out and do not influence our rejection of the null hypothesis regarding sediment nonlinearity. Indeed, if we use the synthetic seismogram ratios (dashed lines in Figure 10) to correct the observed ratios (Figure 4) for the finite source effects, the null hypothesis is still rejected at the 95% confidence level no matter what combination of the four hard-rock sites is used as the reference motion.

4.2. Site Classifications

One final issue concerns how the sites were classified. It is very common for different studies to apply different classifications to a particular site (e.g., based on different geological maps). Furthermore, a subsequent analysis of a site (e.g., a borehole study) often results in a classification change. We have chosen to avoid this thorny issue by adopting the designations given in the Southern California Strong-Motion Database (Table 1) because it represents the most official classification that we could find. However, it is important to note that any wrong classifications in our study will only reduce the average difference due to nonlinearity and will therefore not influence our rejection of the null hypothesis. Nevertheless, it is useful to examine our results for evidence of any miss classifications.

The site response estimate for the soft-rock site LF6 in Figure 2c shows significant amplification. According to *Harmsen* [1997] this site is located on artificial fill and therefore should perhaps be classified as sediment. Of all the weak-motion site response estimates in Figure 2a, that for

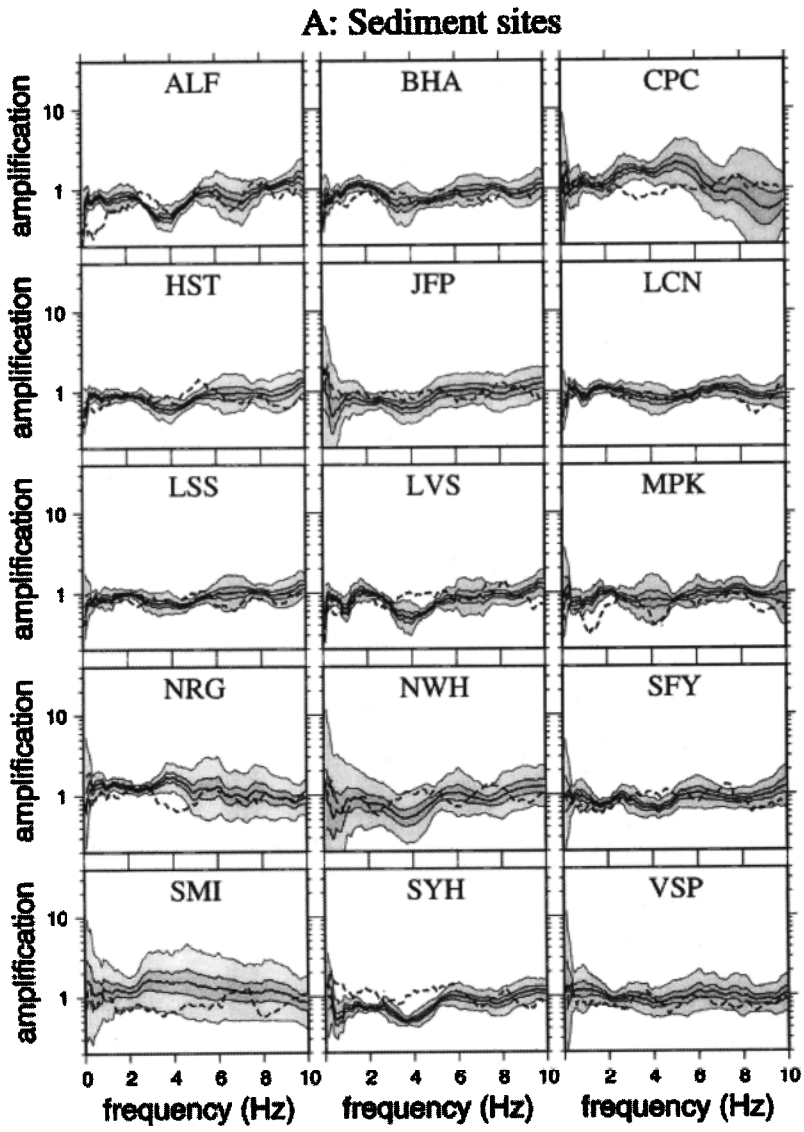

Figure 8. Same as Figures 2a and 2b, except that synthetic seismograms have been used in the analysis as described in the text.

ALF is the only one that does not show significant amplification. In addition, this site plots on the boundary between soft rock (Tertiary units) and sediment (Quaternary alluvium) in the geological map of *Tinsley and Fumal* [1985], so it could be argued that this is in fact a soft-rock site. Finally, the weak-motion site-response estimate for hard-rock site LWS exhibits amplification between 1 and 5 Hz (Figure 2b). In fact, *Hartzell et al.* [1996] resolved three distinct peaks (at ~1.6, ~4.8, and ~8.0 Hz) in their weak-motion estimate for this site, suggesting the fundamental resonant frequency and two higher modes of a sediment layer. Therefore this site should perhaps at least be taken out of the hard-rock category. Making the above three classification changes would only serve to strengthen the rejection of the null hypothesis. To avoid appearing ad hoc, however, we have not made any such classification changes here.

5. Sediment Resonances

Four sites that exhibit a strong sediment resonance in the weak-motion site-response estimates are plotted in Figure 11. These sites were chosen not only because of the apparent resonance but because the peak is also clearly observed in weak-motion horizontal to vertical component spectral ratios (dot-dashed lines in Figure 11), which have previously been shown to effectively reveal the fundamental resonant frequency of sedimentary deposits [*Lermo and Chavez-Garcia*, 1993; *Lachet and Bard*, 1994; *Field and Jacob*, 1995; *Lachet et al.*, 1996; *Seekins et al.*, 1996; *Field*, 1996]. Site NWH has been included, even though the peak is not that much more prominent than those seen at other sites in Figure 2 (e.g., NRG) because the resonance is confirmed by a one-dimensional theoretical prediction based on a borehole drilled at this site (dotted line in Figure 11, see caption for details). Finally, site LF6 (classified as soft rock but perhaps on fill as discussed above) is included because it exhibits clear resonant effects.

For comparison, the main shock site-response estimates are plotted with dashed lines in Figure 11. In all four cases the resonance seen in the weak-motion data is absent in the strong-motion estimate. Because of the natural variability of the weak-motion estimates (represented by the lightly shaded

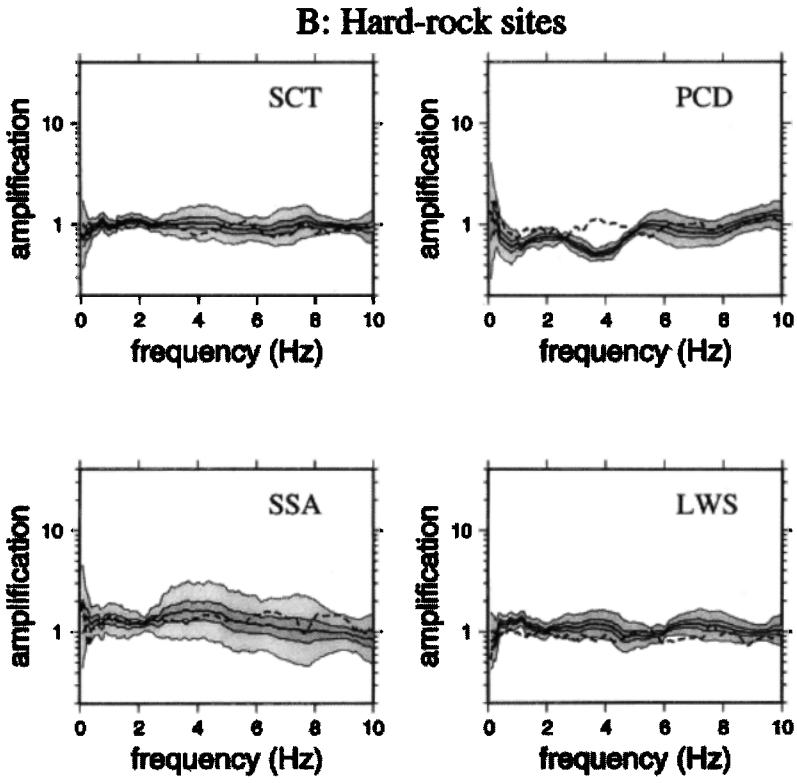

Figure 8. (continued)

region in Figure 2, but not shown in Figure 11) and because of the possible presence of finite source effects in the strong-motion estimates, caution must be exercised in interpreting these results in terms of reduced amplification factors and/or resonant frequency shifts. Nevertheless, the fact that the resonant peak seen clearly in the weak-motion estimates is conspicuously absent in the strong motion data is suggestive of sediment nonlinearity.

6. Discussion and Conclusions

By a systematic comparison of site response estimates between the Northridge earthquake and its aftershocks, we have found it necessary to reject the null hypothesis that sediment response was linear. That is, sediment amplification was significantly reduced, by up to a factor of 2, for the main shock. Although the absolute amplification factors depend somewhat on the reference site definition, the inference of nonlinearity does not. This conclusion is robust with respect to: the exclusion of any possibly anomalous sediment sites if; only aftershocks deeper than 7 km are used; or if the more distant Los Angeles Basin site are considered exclusively.

Kinematic modeling of the main shock ground motion does not suggest any bias from finite source effects. We admit that this and all other methodologies for simulating finite source effects are not totally reliable, especially at higher frequencies. Furthermore, the Northridge-specific rupture model was obtained assuming a linear response at sediment sites [*Zeng and Anderson*, 1996], which we now argue is an invalid assumption. In spite of these limitations the kinematic modeling conducted here does represent the state of the art and is certainly a reasonable, if not totally conclusive, test of finite source effect biases. Using the predictions to correct the observations does not eliminate the significance of nonlinearity, no matter what combinations of rock sites is used to define the reference motion.

This conclusion differs from that of *Harmsen* [1997], who compared spectral amplification of Northridge aftershocks to the average amplification for the 1971 San Fernando, 1987 Whittier Narrows, 1991 Sierra Madre, and 1994 Northridge main shocks. Except for three sites (LF6, SMI, and JFP), all of which he conjectured to have experienced ground failure, he found weak- and strong-motion estimates to be consistent. However, his strong-motion estimates were complicated by including main shock events from widely different epicentral locations. Therefore his ability to infer nonlinearity was exacerbated by the well-known intrinsic variability of site response with respect to source location. We have avoided this problem by examining only the Northridge main shock and its aftershocks, thus enabling the demonstration that nonlinearity was more pervasive than just the three sites that may have experienced ground failure. Similar conclusions have now been reached in other subsequent studies [Beresnev et al., 1998b; Su et al., 1998], which claim to have resolved a trend in the degree of nonlinearity as a function of input motion level.

That the nonlinearity observed here is greatest at ~3 Hz, and reduced at higher frequencies, appears to contradict the laboratory observation that damping values increase (or Q decreases) with increasing strain levels (implying an increasing discrepancy with frequency). However, fully nonlinear calculations predict a transition frequency above which amplification is actually increased by the nonlinear response [e.g., *Yu et al.*, 1993]. This previously unanticipated

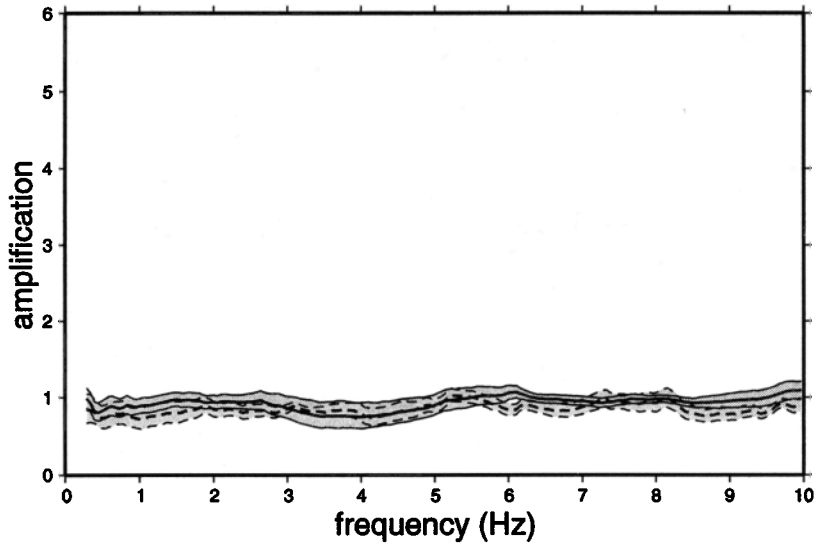

Figure 9. Same as Figure 3, except that synthetic seismograms have been used in the analysis as described in the text.

behavior is now understood as a manifestation of period doubling and sum-and-difference frequency interactions, which have been observed in the laboratory and are well understood in terms of classic perturbation theory [e.g., *Johnson et al.*, 1996]. Another explanation is that laboratory studies do not include the effects of scattering attenuation, which may already dominate the high frequency response at deep soil sites (this would explain the low weak-motion amplification levels implied by Figure 3 at higher frequencies).

In order to infer the presence of nonlinearity we were forced to combine the observations from several sediment sites, each of which experienced a different and unknown level of input motion during the main shock In addition, each of the sites has its own unique, and generally poorly understood, sediment structure and composition. Therefore it is difficult to make quantitative statements about the degree of nonlinearity as a function of input motion or site type, other than to say that it is significant at sediment sites near where peak ground accelerations between ~300 and ~425 cm/s^2 were observed at hard-rock sites. It is even more difficult to learn anything about the underlying physical mechanisms from our study.

From a seismologist's perspective, therefore, this study represents the logical first step in answering the long-standing question regarding nonlinear effects at sediment sites in the Los Angeles region. However, as discussed by *Field et al.* [1998], we are still a long way from testing the laboratory-based engineering methodologies used routinely in practice or from understanding the physics of nonlinear sediment response in terms of equation of state relationships and physical mechanisms. More research is clearly needed, and progress may well depend on the collection of more strong-motion data. By far the most effective strategy will be the use

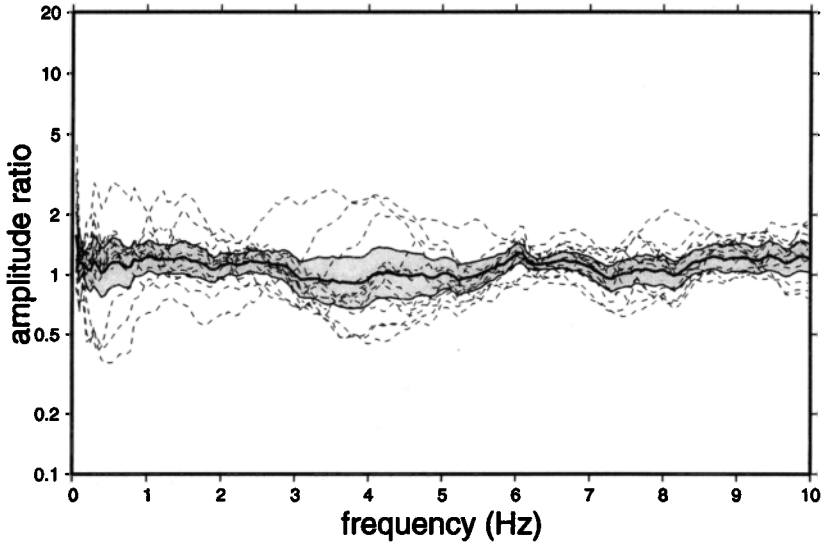

Figure 10. Same as Figure 4, except that synthetic seismograms have been used in the analysis as described in the text. The three anomalously low ratios below 1 Hz represent rupture directivity effects at NWH, JFP, and SYH.

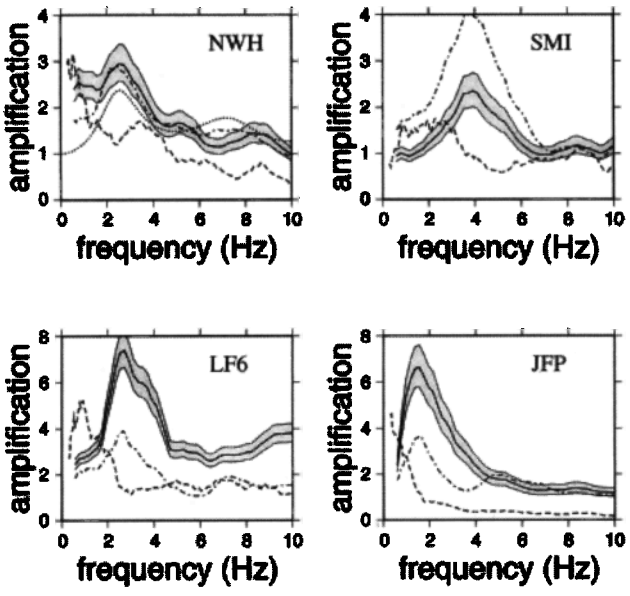

Figure 11. Site response estimates at four sites that reveal a clear fundamental resonance in the weak-motion estimate (solid lines with 95% confidence intervals shaded). The dot-dashed lines represent average horizontal to vertical component spectral ratios, and the dotted line for NWH is the predicted one-dimensional weak-motion shear wave site response based on a borehole study at the site (preliminary data from the "Resolution of Site Response Issues from the Northridge Earthquake" project; C. Roblee, personal communication, 1997). The horizontal to vertical component spectral ratios, and the theoretical prediction, provide independent evidence that the observed peaks represent a fundamental resonance of the sediments. That the peaks are clearly absent, or at least shifted, in the strong motion estimates (dashed lines), suggests a nonlinear response during the main shock.

of borehole arrays which, as demonstrated by *Wen et al.* [1994, 1995] and *Kazama* [1996], are very effective in resolving resonant-frequency shifts and reducing uncertainties associated with the input motion.

One immediate geophysical implication of this study is that the use of empirical Green's functions (i.e., small earthquakes) as an estimate of the combined path and site effects for large earthquakes may be inappropriate at sediment sites. For example, the inference of source properties for large earthquakes using empirical Green's function deconvolution [*Bakun and Bufe*, 1975; *Mueller*, 1985] may give biased results if nonlinear effects are present. In addition, the use of empirical Green's functions in composite source simulations of large earthquakes [e.g., *Irikura*, 1983; *Hutchings*, 1994] may overpredict ground motion at sediment sites. We plan to test this latter assertion using the Northridge data in a future study.

Appendix: Spectral Estimation Procedure

Since a variety of sensor types were used to collect the data, the time series were instrument corrected and converted (if necessary) to acceleration. After a visual inspection to remove data containing any instrument problems, the seismograms were windowed with a 20 s segment starting 1 s before the shear wave arrival. Fourier amplitude spectra were then computed and smoothed with a boxcar function that increased in width with the log of frequency (e.g., 0.5 Hz width at 1 Hz and 1.3 Hz width at 10 Hz).

Aftershock spectral values were eliminated from consideration for any one of the following reasons: (1) they did not exceed 2.7 times that of the noise measured from the pre-*P* wave signal; (2) the frequency was less than one-fourth that of the natural period of the seismometer (if recorded with a velocity sensor); or (3) the hypocentral distance was less than 10 km (to minimize the effect of location uncertainties in the path-effect correction). Finally, all of the remaining horizontal component observations for a given site and event (some of the sites recorded on more than one type of sensor and/or gain level) were combined with a geometric average.

Acknowledgments. We are indebted to Koen Van Den Abeele for numerous helpful discussions. We also thank Robert Guyer and members of the Institute for Crustal Studies (UCSB) for constructive comments. The data used in this study were collected by SCEC, the U.S. Geological Survey, the California Division of Mines and Geology, the University of Southern California, the Department of Energy, and the City of Los Angeles. This work was funded in part by Institutional Support from Los Alamos (LDRD) through the Office of Basic Energy Science (Engineering and Geoscience). E. H. Field received support from the U.S. Geological Survey under grant no. 1434-97-GR03196.

References

Aguirre, J., and K. Irikura, Preliminary analysis of non-linear site effects at Port Island array station during the 1995 Hyogoken-Nambu earthquake, *J. Nat. Disaster Sci., 16*, 49-58, 1995.

Aki, K., Local site effects on strong ground motion, *Earthquake Engineering and Soil Dynamics*, edited by J. Lawrence Von Thon, vol. II, pp. 103-155, Am. Soc. Civ. Eng., New York, 1988.

Aki, K., Local site effects on weak and strong ground motion, *Tectonophysics, 218*, 93-111, 1993.

Andrews, D.J., Objective determination of source parameters and similarity of earthquakes of different size, in *Earthquake Source Mechanics*, Geophys. Monogr. Ser., vol. 37, edited by S. Das, J. Boatwright, and C.H. Scholz, pp. 259-268, Washington, D.C., 1986.

Archuleta, R.J., and S.H. Hartzell, Effects of fault finiteness on near-source ground motion, *Bull. Seismol. Soc. Am., 71*, 939-957, 1981.

Bakun, W.H., and C.G. Bufe, Shear wave attenuation along the San Andreas Fault zone in central California, *Bull. Seismol. Soc. Am., 65*, 439-459, 1975.

Beresnev, I.A. and K.L. Wen, Nonlinear soil response--A reality?, *Bull. Seismol. Soc. Am., 86*, 1964-1978, 1996.

Beresnev, I.A., E.H. Field, P.A. Johnson, and K. E.-A. Van Den Abeele, Magnitude of nonlinear sediment response in Los Angeles basin during the 1994 Northridge, California earthquake, *Bull. Seismol. Soc. Am.*, 99, 1079-1084, 1998a.

Beresnev, I.A., G.M. Atkinson, P.A. Johnson, and E.H. Field, Stochastic finite-fault modeling of ground motions from the 1994 Northridge, California earthquake: II widespread nonlinear response at soil sites, *ull. Seismol. Soc. Am.*, in press, 1998b.

Boatwright, J., J.B. Fletcher, and T.E. Fumal, A general inversion scheme for source, site, and propagation characteristics using multiply recorded sets of moderate-sized earthquakes, *Bull. Seismol. Soc. Am., 81*, 1754-1782, 1991.

Bonamassa, O., and C.S. Mueller, Source and site response spectra from the aftershock seismograms of the Whittier Narrows, California, earthquake, *Seismol. Res. Lett., 59*, 23, 1989.

Bonilla, L.F., J.H Steidl, G. T. Lindley, A.G. Tumarkin, and R.J. Archuleta, Site Amplification in the San Fernando Valley, CA: Variability of site effect estimation using the *S*-wave, coda, and H/V methods, *Bull. Seismol. Soc. Am., 87*, 710-730, 1997.

Borcherdt, R.D., Effects of local geology on ground motion near San Francisco Bay, *Bull. Seismol. Soc. Am., 60*, 29-61, 1970.

Borcherdt, R.D., Preliminary amplification estimates inferred from strong ground motion recordings of the Northridge earthquake of

January 17, 1994, paper presented at the International Workshop on Site Response Subjected to Strong Earthquake Motion, Port Harbour Res. Inst., Yokusaka, Japan, Jan. 16-17, 1996.

Celebi, M., J. Prince, C. Dietel, M. Onate, and G. Chavez, The culprit in Mexico City - Amplification of motions, *Earthquake Spectra, 3*, 315-328, 1987.

Chang, S.W., J.D. Bray, and R.B. Seed, Engineering implications of ground motions from the Northridge earthquake, *Bull. Seismol. Soc. Am., 86*, S270-S288, 1996.

Chin, B., and K. Aki, Simultaneous study of the source, path, and site effects on strong ground motion during the 1989 Loma Prieta earthquake: A preliminary result on pervasive nonlinear site effects, *Bull. Seismol. Soc. Am., 81*, 1859-1884, 1991.

Chin, B.-H., and K. Aki, Reply to "Comment on Simultaneous study of the source, path, and site effects on strong ground motion during the Loma Prieta earthquake: A preliminary result on pervasive nonlinear effects" by L. Wennerberg, *Bull. Seismol. Soc. Am., 86*, 268-273, 1996a.

Chin, B.-H. and K. Aki, Local site effects study on ground motion during the 1994 Northridge Earthquake, paper presented at the International Workshop on Site Response Subjected to Strong Earthquake Motion, Port Harbour Res. Inst., Yokusaka, Japan, Jan. 16-17, 1996b.

Edelman, A., and F. Vernon, The Northridge portable instrument aftershock data set, *SCEC Data Product Rep.* , Univ. of Calif., San Diego, 1995.

Field, E.H., Spectral amplification in a sediment-filled valley exhibiting clear basin-edge induced waves, *Bull. Seismol. Soc. Am., 86*, 991-1005, 1996.

Field, E.H., and K.H. Jacob, A comparison and test of various site response estimation techniques, including three that are not reference site dependent, *Bull. Seismol. Soc. Am., 85*, 1127-1143, 1995.

Field, E.H., P.A. Johnson, I.A. Beresnev, and Y. Zeng, Nonlinear ground-motion amplification by sediments during the 1994 Northridge earthquake, *Nature, 390*, 599-602, 1997.

Field, E.H., S. Kramer, A.-W. Elgamal, J.D. Bray, N. Matasovic, P.A. Johnson, C. Cramer, C. Roblee, D.J. Wald, L.F. Bonilla, P.P. Dimitriu, and J.G. Anderson, Nonlinear site response: Where we're at, *Seismol. Res. Lett.*, In Press, 1998.

Finn, W.D.L., Geotechnical engineering aspects of microzonation, Paper presented at Fourth International Conference on Seismic Zonation, Earthq. Eng. Res. Inst, Stanford, Calif., 1991.

Hardin, B.O., and V.P. Drnevich, Shear modulus and damping in soils: Measurement and parameter effects, *J. Soil Mech. Found. Div. Am. Soc. Civ. Eng., 98*, 603-624, 1972a.

Hardin, B.O., and V.P. Drnevich, Shear modulus and damping in soils: Design equations and curves, *J. Soil Mech. Found. Div. Am. Soc. Civ. Eng., 98*, 667-692, 1972b.

Harmsen, S.C., Determination of site amplification in the Los Angeles urban area from inversion of strong-motion records, *Bull. Seismol. Soc. Am., 87*, 866-887, 1997.

Hartzell, S, A. Leeds, A. Frankel, and J. Michael, Site response for urban Los Angeles using aftershocks of the Northridge earthquake, *Bull. Seismol. Soc. Am., 86*, S168-S192, 1996.

Heaton, T.H., The 1971 San Fernando earthquake; A double event?, *Bull. Seismol. Soc. Am., 72*, 2037-2062, 1982.

Heaton, T.H., Evidence for and implications of self-healing pulses of slip in earthquake rupture, *Phys. Earth Planet Inter., 64*, 1-20, 1990.

Hutchings, L., Kinematic earthquake models and synthesized ground motion using empirical Green's functions, *Bull. Seismol. Soc. Am., 84*, 1028-1050, 1994.

Idriss, I.M, Response of soft soil sites during earthquakes, *Proc. H. Bolton Seed Memorial Symposium*, edited by J.M. Duncan, pp. 273-290, BiTech Publ., Berkely, Calif., 1990.

Irikura, K., Semi-empirical estimation of strong ground motions during large earthquakes, *Bull. Disaster Prev. Res. Inst. Univ. Kyoto, 33*, 63-104, 1983.

Ishihara, K., *Soil Behavior in Earthquake Geotechnics*, Oxford Univ. Press, New York, 1996.

Jarpe, S.P., L.J. Hutchings, T.F. Hauk, and A.F. Shakal, Selected strong- and weak-motion data from the Loma Prieta earthquake sequence, *Seismol. Res. Lett., 60*, 167-176, 1989.

Johnson, P.A., B. Zinszner, and P.N.J. Rasolofosaon, Resonance and nonlinear elastic phenomena in rock, *J. Geophys. Res., 101*, 11553-11564, 1996.

Kazama, M., Nonlinear dynamic behavior of the ground inferred from strong motion array records at Kobe Port Island during the 1995 Hyogo-Ken Nanbu Earthquake, paper presented at the International Workshop on Site Response Subjected to Strong Earthquake Motion, Port Harbour Res. Inst., Yokusaka, Japan, Jan. 16-17, 1996.

Lachet, C., and P.-Y. Bard, Numerical and theoretical investigations on the possibilities and limitations of Nakamura's technique, *J. Phys. Earth, 42*, 377-397, 1994.

Lachet, C., D. Hatzfield, P.-Y. Bard, N. Theodulidis, C. Papaioannou, and A. Savvaidis, Site effects and microzonation in the City of Thessaloniki (Greece): Comparison of different approaches, *Bull. Seismol. Soc. Am., 86*, 1692-1703, 1996.

Lermo, J., and F.J. Chavez-Garcia, Site effect evaluation using spectral ratios with only one station, *Bull. Seismol. Soc. Am., 83*, 1574-1594, 1993.

Luco, J.E. and R.J. Apse, On the Green's functions for a layered half-space, part I, *Bull. Seismol. Soc. Am., 73*, 909-929, 1983.

Meremonte, M., A. Frankel, E. Cranswick, D. Carver, and D. Worley, Urban seismology--Northridge aftershocks recorded by multiscale arrays of portable digital seismographs, *Bull Seismol. Soc. Am., 86*, 1350-1363, 1996.

Milne, J., *Seismology*, 1st ed., Kegan Paul, Trench, Truber, London, 1898.

Mueller, C.S., Source pulse enhancement by deconvolution of an empirical Green's function, *Geophys. Res. Lett., 12*, 33-36, 1985.

Peng, J.Y., Spatial and temporal variation of coda Q in California, Ph.D. Thesis, Univ. of South. Calif., Los Angeles, 1989.

Petersen, M.D., W.A. Bryant, C.H. Cramer, M.S. Reichle, and C.R. Real, Seismic ground-motion hazard mapping incorporating site effects for Los Angeles, Orange, and Ventura counties, *Bull. Seismol. Soc. Am., 87*, 249-255, 1997.

Rial, J.A., The anomalous seismic response of the ground at the Tarzana hill site during the Northridge 1994 Southern California earthquake: A resonant, sliding block?, *Bull. Seismol. Soc. Am., 86*, 1714-172, 1996.

Rogers, A.M., R.D. Borcherdt, P.A. Covington, and D.M. Perkins, A comparative ground response study near Los Angeles using recordings of Nevada nuclear tests and the 1971 San Fernando earthquake, *Bull. Seismol. Soc. Am., 74*, 1925-1949, 1984.

Sato, T., and T. Hirasawa, Body wave spectra from propagating shear crocks, *J. Phys. Earth, 21*, 415-431, 1973.

Seed, H.B., and I.M Idriss, Ground motions and soil liquefaction during earthquakes, report, Earthquake Eng. Res. Inst., El Cerrito, Calif., 1983.

Seed, H.B., and K.L. Lee, Liquefaction of saturated sands during cyclic loading, *J. Am. Soc. Cil. Eng., 92* (SM6), 105-134, 1966.

Seekins, L.C., L. Wennerberg, L. Margheriti, and H.-P. Liu, Site amplification at five locations in San Francisco: A comparison of *S*-waves , codas, and microtremors, *Bull. Seismol. Soc. Am., 86*, 627-635, 1996.

Somerville, P.G., N.F. Smith, R.W. Graves, and N.A. Abrahamson, Modification of empirical strong ground motion attenuation relations to include the amplitude and duration effects of rupture directivity. *Seismol. Res. Lett., 68*, 199-222, 1997.

Spudich, P., M. Hellweg, and W.H.K. Lee, Directional topographic site response at Tarzana observed in aftershocks of the 1994 Northridge, California, earthquake: Implications for main shock motions, *Bull. Seismol. Soc. Am., 86*, S193-S208, 1996.

Su, F., J.G. Anderson, and Y. Zeng, Study of weak and strong ground motion including nonlinearity from the Northridge, California, earthquake sequence, *Bull. Seism. Soc. Am.*, in press, 1998.

Tinsley, J.C., and T.E. Fumal, Mapping Quaternary sedimentary deposits for areal variations in shaking response, in *Evaluating Earthquake Hazards in the Los Angeles region-An Earth-Science Perspective, U.S. Geol. Surv. Prof. Pap., 1369*, 101-125, 1985.

Vucetic, M., and R. Dobry, Effect of soil plasticity on cyclic response, *J. Geotech. Eng., 117*, 89-107, 1991.

Wald, D.J., T.H. Heaton, and K.W. Hudnut, The slip history of the 1994 Northridge, California earthquake determined from strong-motion, teleseismic, GPS, and leveling data, *Bull. Seismol. Soc. Am., 86*, S49-S70, 1996.

Wen, K.-L., I.A. Beresnev, and Y.T. Yeh, Nonlinear soil amplification inferred from downhole strong seismic motion data, *Geophys. Res. Lett., 21*, 2625-2628, 1994.

Wen, K.-L., I.A. Beresnev, and Y.T. Yeh, Investigation of nonlinear

site amplification at two downhole strong ground motion arrays in Taiwan, *Earthquake Eng. Struct. Dyn.*, *24*, 313-324, 1995.

Wennerberg, L., Comment on "Simultaneous study of the source, path, and site effects on strong ground motion during the Loma Prieta earthquake: A preliminary result on pervasive nonlinear effects" by B.-H Chin and K. Aki, *Bull. Seismol. Soc. Am.*, *86*, 259-267, 1996.

Yu, G., J.G. Anderson, and R. Siddharthan, On the characteristics of nonlinear soil response, *Bull. Seismol. Soc. Am.*, *83*, 218-244, 1993.

Zeng, Y., and J.G. Anderson, A composite source model of the 1994 Northridge earthquake using genetic algorithms, *Bull. Seismol. Soc. Am.*, *86*, S71-S83, 1996.

Zeng, Y., J.G. Anderson, and G. Yu, A composite source model for computing realistic synthetic strong ground motion, *Geophys. Res. Lett.*, *21*, 725-728, 1994.

I. Beresnev, Department of Earth Sciences, Carleton University, 1125 Colonel By Drive, Ottawa, Ontario, Canada K1S 5B6. (e-mail: beresnev@ccs.carleton.ca)

E. Field, Department of Earth Sciences, University of Southern California, Los Angeles, CA 90089-0740. (e-mail: field@usc.edu)

P. Johnson, Los Alamos National Laboratory, Los Alamos, NM, 87545. (e-mail: johnson@seismo5.lanl.gov)

Y. Zeng, Seismological Laboratory, University of Nevada, Reno, NV, 89557. (e-mail: zeng@seismo.unr.edu)

(Received December 8, 1997; revised May 14, 1998;
accepted June 19, 1998.)